HHS Public Access

Author manuscript

Biofabrication. Author manuscript; available in PMC 2016 September 01.

Published in final edited form as:

Biofabrication. ; 7(3): 035005. doi:10.1088/1758-5090/7/3/035005.

Computer Aided Biomanufacturing of Mechanically Robust Pure Collagen Meshes with Controlled Macroporosity

Anowarul Islam[1], **Katherine Chapin**[2], **Mousa Younesi**[1], and **Ozan Akkus**[1,2,3,*]

[1]Department of Mechanical and Aerospace Engineering, Case Western Reserve University, Cleveland, OH 44106

[2]Department of Biomedical Engineering, Case Western Reserve University, Cleveland, OH 44106

[3]Department of Orthopaedics, Case Western Reserve University School of Medicine, Cleveland, OH 44106

Abstract

Reconciliation of high strength and high porosity in pure collagen based structures is a major barrier in collagen's use in load-bearing applications. The current study developed a CAD/CAM based electrocompaction method to manufacture highly porous patterned scaffolds using pure collagen. Utilization of computerized scaffold design and fabrication allows the integration of mesh-scaffolds with controlled pore size, shape and spacing. Mechanical properties of fabricated collagen meshes were investigated as a function of number of patterned layers, and with different pore geometries. The tensile stiffness, tensile strength and modulus ranges from 10-50 N/cm, 1-6 MPa and 5-40 MPa respectively for all the scaffold groups. These results are within the range of practical usability of different tissue engineering application such as tendon, hernia, stress urinary incontinence or thoracic wall reconstruction. Moreover, 3-fold increase in the layer number resulted in more than 5-fold increases in failure load, toughness and stiffness which suggests that by changing the number of layers and shape of the structure, mechanical properties can be modulated for the aforementioned tissue engineering application. These patterned scaffolds offer a porosity ranging from 0.8-1.5 mm in size, a range that is commensurate with pore sizes of repair meshes in the market. The connected macroporosity of the scaffolds facilitated cell-seeding such that cells populated the entire scaffold at the time of seeding. After 3 days of culture, cell nuclei became elongated. These results indicate that the patterned electrochemical deposition method in this study was able to develop mechanically robust, highly porous collagen scaffolds with controlled porosity which not only tries to solve one of the major tissue engineering problems in a fundamental level but also has a significant potential to be used in different tissue engineering applications.

Introduction

Collagen is at the center of many tissue engineering strategies. It is a ubiquitous molecule that can be extracted from animal tissues. Generally, collagen is well tolerated in

Correspondence to: Ozan Akkus.

*Author of correspondence

vivo[27, 38, 46]. It presents cell adhesion sites and it can be digested enzymatically by cellular action. Owing to such favorable properties, collagen is used in many clinical applications[6, 8, 24, 25, 54, 64]. While pure collagen scaffolds present advantages in terms of cell response, they are weak and their use is mostly limited to non-load bearing applications such as barrier sheets, hemostatic chips and sponges to fill cavities[2, 7, 13, 23, 63, 71-73]. Therefore, biofabrication modalities that would increase the mechanical robustness of collagen-based materials would expand the spectrum of applications for collagen.

Another challenge associated with collagen biofabrication is the introduction of porosity. Porosity is essential for tissue integration and neo-vascularization. However, at the same time, porosity intrinsically reduces the mechanical strength of scaffolds. Classically, porosity is induced by freeze drying or salt-leaching[30, 35, 56]. While these methods are useful, porosity is random, has limiting interconnectedness and degree of control on the uniformity of pore size and shape is low. Furthermore, most applications which require tissue integration and vascularization require macroscale porosity (0.5 mm or greater)[31]. Therefore, it is a major challenge to reconcile macroporosity with mechanical robustness in delicate protein-based biomaterials such as collagen.

Recent years have seen the introduction of the electrochemical compaction of collagen molecules to manufacture condensed tissue-analog forms[1, 16, 74]. In this approach, electrical currents are applied to collagen solutions. The resulting pH gradient in the solution results in the repulsion of collagen molecules by both electrodes and molecules become compacted between the electrodes. The electrocompaction method has been used for high strength collagen threads by using parallel wire electrodes[4, 81]. In this study we developed a novel biofabrication method to manufacture patterned pore-lattice structures with controlled size and shape by computer-aided electrocompaction of collagen molecules using electrical currents. The aims of this study are: 1) to demonstrate the capabilities of patterned electrocompaction method in manufacturing scaffolds with different pore size and shapes; 2) report on mechanical characteristics of resulting scaffolds, 3) demonstrate the propensity of the macroporous scaffold for cell-seeding.

Materials and Method

Overview of the Patterned Electrocompaction Process (Figure 1)

The method requires two planar carbon electrodes (each approximately 25×25 mm) for patterned deposition. A polycarbonate sheet of 2 mm in thickness is glued on the cathode using cyanoacrylate. This bilayered structure is then mounted on a computer controlled micromill (Sherline CNC, Haverford CA). The negative replica of the desired pattern is designed in CAD environment (Solidworks) and it is machined on the plastic sheet in full depth to expose the underlying cathode's surface. The channels machined within the polycarbonate layer as such are later filled with the collagen solution to be electrocompacted.

Manufacturing an individual patterned layer

Acid soluble monomeric collagen solution (bovine dermis, Advanced Biomatrix, CA; 6 mg/ml) was diluted two-fold, pH was adjusted between 8-10 using 1N NaOH and dialyzed against ultrapure water for 18 hours. Dialyzed collagen was loaded in the patterned groves of the machined plastic-cathode bilayer by applying with a syringe. The carbon anode layer was placed on the top of the plastic-cathode bilayer. 30 VDC was applied for 2 min. across the electrodes. This results in electrophoretic compaction of collagen molecules within the patterned groove. The width of the groove was 1 mm for all of the scaffold groups. The biophysical mechanisms causing the electrocompaction of molecules were explained and discussed in detail before[16, 74]. Briefly, electrical current generates acidic conditions near the anode and basic pH near the cathode. Collagen has positive and negative net charge under acidic and basic conditions, respectively. These charges are similar to the charges of the electrodes to which the molecules are close to, resulting in the repulsion of molecules from both electrodes. The net effect of repulsion is the compaction of molecules as a dense layer. Following electrocompaction, the plastic-cathode bilayer with the collagen deposit is recovered.

Three different pore geometries were manufactured to demonstrate the control on pore morphology: i) rectangular ii) square and iii) diamond. The average pore sizes for rectangular, square and diamond-shaped scaffolds are 1.5, 0.8 and 1.2 mm with corresponding porosities of 55%, 43% and 61%, respectively. To assess the effect of pore geometries on the mechanical properties of the scaffold, another pore architecture with parallel pore channels (group iv) with intermittent connections was manufactured. The parallel channel pore scaffold group has 53% porosity which is comparable to rectangular and diamond shape pore scaffold.

The computerization of the process allowed for fabrication of multiple layers in one electrode platform as shown here (Figure 2A&B). The lattice structure can be designed to control the width of the channels and the spacing between them. An increased spacing or reduced channel width resulted in greater pore volume. The lattice was cast in a fashion to include a rectangular frame at the perimeter which to allow for recovering and handling the patterned deposit. The frame was also helpful in registering multiple patterned sheets to make multilayered scaffolds.

Fabrication of 3-D Scaffolds with Controlled Interconnected Porosity

The individual patterned layers were stacked on top of each other in register to obtain the final scaffold as shown in Figure 2A&B. Collagen solution (6 mg/mL, pH = 6) was brushed between layers as a binder prior to stacking the layers. The layered structure was kept under load under a deadweight for an hour, placed in 1x PBS at 37 °C for 6 hours to induce fibrillogenesis as we have shown before[75]. Scaffolds were stored in 2-propanol solution when not used. Scaffolds were crosslinked in 0.625% genipin (Wako Chemical, Japan) in 90% v/v ethanol solution at 37 °C for 3 days[4].

To evaluate the effect of number of layers on the overall mechanical properties of the scaffold, square pore scaffolds with 3 different layer numbers: v) 2 layers vi) 4 layers and

vii) 6 layers were manufactured. The lateral dimensions of the individual layer as well as the final scaffolds were 20 × 12 mm.

Imaging of Molecular Alignment within Patterned Channels

After manufacturing the patterned layer, the molecular alignment of collagen molecules within the electrocompacted pattern was examined by a polarized optical microscope (Olympus BX51, Melville, NY, USA) and a first order wavelength gypsum plate. Collagen is a positive birefringent material, where the molecules which are aligned along the slower axis of this plate shows blue interference color and the molecules which are perpendicular to the slow axis appear yellow[44]. Magenta color indicates lack of alignment and blue color indicates alignment of the collagen molecule along the slower axis or perpendicular to the long dimension of the gypsum plate.

Assessment of Mechanical Properties of Patterned Bioscaffolds

Patterned scaffolds with different pore geometries and different layer numbers (N = 6/group) were tested under monotonic tension until failure using a displacement rate of 10 mm/min (RSA II, Rheometrics Inc., Piscataway, NJ, USA). Scaffolds were hydrated in water for 30 min prior to testing. The ends of the scaffolds were gripped by tensile fixture at a gauge length of 10 mm. A 10 N load-cell was used to measure the load. The thickness of the scaffolds was measured by a custom-made micrometer where the micrometer closes an electrical circuit and makes an audible sound in a multimeter when touches the surface of wet scaffolds. Load values were normalized with the wet cross sectional area and displacement values were normalized by the gage length to obtain stress-strain plots. Area is calculated as the product of number of collagen filament in the tensile direction, width of the filaments and average thickness of the filaments in the tensile direction of the scaffolds. Failure load, stiffness, elastic modulus, failure stress and toughness were calculated from stress-strain curves. Elastic modulus and stiffness were calculated at the steepest region of the stress strain curves. Toughness was calculated as the area under the stress-strain curves.

Adhesion and morphology of human mesenchymal stem cells seeded on patterned bioscaffolds

To demonstrate that the 3D-controlled porosity enables cell-loading throughout the continuum of the patterned scaffold, cells were seeded on 6-layered scaffolds (10 mm X 5 mm X 0.5 mm, rectangular porosity with 1.5 mm pore size) following sterilization in 70% ethanol overnight. Scaffolds were placed in an ultralow attachment 24-well plate (1 scaffold/well). Human mesenchymal stem cells (Lonza, Walkersville, MD) were seeded at a density of 250,000 cells/well. The culture medium was composed of alpha MEM (Invitrogen) supplemented with 10% MSC-FBS (Invitrogen), 1% penicillin/streptomycin and 50 μg/mL ascorbic acid. Twelve hours after seeding, the unattached cells were removed by replacing the growth medium and the cells adherent on the scaffolds were cultured for 3 days. Cell morphology was visualized by staining the cell actin filaments using AlexaFluor 488 Phalloidin (Life Technologies, Grand Island, NY, USA) at day 3. Briefly, cells were fixed with 3% formaldehyde (with 0.1% TritonX-100) for 10 min and washed with 1x PBS. The actin filaments were stained by incubating the cells in AlexaFluor 488 Phalloidin at 37 °C for 20 min. The stain was washed with 1x PBS and images of actin stained cells were taken

using an Olympus Microscope. To visualize the cell nucleus, DAPI nucleic acid staining (Invitrogen) was also performed after day 3.

Statistical Analysis

A one-way analysis of variance (ANOVA) test was performed to evaluate for significant differences between groups. Two sets of groups were analyzed separately for significant difference within the groups. The first set was different pore geometries groups: i) rectangular ii) square iii) diamond-shaped pore and iv) parallel channel pore. The second set was square pore scaffolds with: v) 2 layers vi) 4 layers and vii) 6 layers. Significant differences between means were calculated and significance level was set at $p < 0.05$. A *post-hoc* analysis using the Tukey's test was conducted to compare pairwise differences between groups.

Results

Four types of patterned lattice structures were fabricated (Fig. 4). The collagen filaments of the scaffold with diamond-shaped pores lacked alignment (magenta in CPI image in Fig. 3A). In contrast, the scaffolds which are fabricated with parallel filaments had collagen molecules aligned parallel to the longer axes of the filaments as evidenced by blue coloration (Fig. 3B).

The typical stress-strain plots of scaffolds with increasing number of layers (group v, vi and vii) showed that 2-layered scaffold failed abruptly with limited plastic deformation. 4-layered and 6-layered groups showed prominent post-yield deformability (Fig. 5a).

There was a non-linear increase in the structural mechanical properties of scaffolds with increasing number of layers. Such that, 3-fold increase (2 layer to 6 layer) in the number of layers resulted in increases in more than 3-fold increase in failure load (7-fold), toughness (5.5-fold) and stiffness (7- fold) (Fig. 5b-f).

The stress-strain plots of the different porosity geometry shape showed that the scaffolds with diamond-shaped pores failed more abruptly than square/rectangular shape pore and parallel channel pore scaffolds (Fig. 6a). Failure stress, elastic modulus, stiffness and toughness were highest for rectangular/square-shaped pore scaffolds, intermediate for parallel channel pore scaffolds and lowest for diamond-shaped pore scaffolds and these properties increased about 6-fold, 7-fold, 2.5-fold and 8-fold respectively from diamond-shaped pore scaffold to square shape pore scaffold (Fig. 6b-f). There were no significant differences between the material properties of rectangular and square-shaped pore scaffolds (Fig. 6b-f).

F-actin and DAPI stained images taken from fields of view located in the deeper layers of scaffolds (Fig. 7) revealed that cells were uniformly seeded over the filaments. Actin cytoskeleton of cells was elongated along the longer axis of the threads. The nuclei also became elongated along the length of the collagen filament in the scaffolds (Fig. 7) with a nuclear aspect ratio of 2.15 ± 0.34 after 3 days of culture.

Discussion

A novel method of manufacturing, patterned planar electrochemical compaction of pure collagen was developed. The method fabricated mechanically promising patterned scaffolds with controlled porosity. Different pattern types were generated to show the versatility of the fabrication. The process involved the design of desired pore configuration via computer aided design and the machining of the pattern by computer controlled numerical machine tool. These computational modalities provided the control over 3D scaffold morphology.

There are several methods to prepare porous three-dimensional biodegradable scaffolds, including gas foaming[29, 52], phase separation[53, 67, 68], porogen leaching[49, 50], fiber extrusion and bonding[48], emulsion freeze-drying,[78] and solid free-form fabrication (SFF) such as 3-D printing[32, 69], bioplotting[41, 42, 79], selective laser sintering[65]. Gas foaming process may produce structure with largely unconnected pores and a non-porous external surface. Particulate leaching is limited for thicker scaffolds, phase separation is limited by the number of materials included in the formulation, and SFF of collagen generally requires the inclusion of secondary polymers to provide consistency. SFF also require expensive specialized instruments and mass production via SFF may present challenges. Electrospinning and fiber meshes uses fibers to make porous structure. However, electrospinning uses toxic solvents and control over pore size and shape is not possible. Moreover electrospinning and other techniques usually utilize a secondary synthetic polymer besides the collagen to enable manufacturability [15, 19, 39, 47, 61]. Freeze drying provides porous collagen scaffolds and pore size and elongation can be controlled to some extent [28, 30, 56, 66]. On the other hand, freeze drying process generally produces weak structures with elastic modulus and failure stress values in the kPa range[62]. There is no single technique which can provide mechanically robust pure collagen based 3-D scaffolds with controlled porosity. The demonstrated electrocompaction method addresses this limitation to a significant extent. Importantly, the method lends itself to scaled-up production by using arrays of electrodes over large surface areas.

Mechanical test results of different pattern types and layer numbers suggest that the patterned scaffold manufactured by the method in this study has a potential to be used in the biomaterials and tissue engineering fields where strength and controlled porosity is required. The enhancement in mechanical properties is largely associated with the ability of the method to compact the pure monomeric collagen to solid phase within the channels of the cathode (Fig. 1A). Prior studies from our group demonstrated up to 300 fold increase in packing density of collagen (3 mg/mL to 1030 mg/mL)[20] molecules. The alignment of collagen molecules along the length of the channels also contributes to mechanical robustness.

Increasing the layer number has a disproportionately greater benefit on the mechanical properties of meshes. From 2 layer to 4 layer scaffold the failure load increased about 2.5 fold whereas from 2 layer to 6 layer scaffold it increased about 7 fold. Similarly, stiffness and toughness increased 7 fold and 5.5 fold respectively from 2 layer to 6 layer. Two-layer scaffolds failed abruptly at the end of the linear elastic region while as the layer number increased, the 4-layered and 6-layered scaffolds showed prominent post yield deformability.

This increase is mechanical properties and prominent post yield deformability in increasing layer numbers may be a result of additional layers complementing the weak points in other layers. This support, in turn, results in a nonlinear increase in the mechanical properties with increasing number of layers. This result also indicates that layer numbers can be increased as an option to match the strength of native tissues.

There were variations between mechanical properties for variation of pattern type (e.g. rectangular/square- shaped pore, parallel channel pore and diamond-shaped pore). Diamond-shaped pore scaffold showed significantly inferior mechanical performance than the other types of scaffold. This outcome was associated with lack of molecular alignment in the diamond-shaped patterned pores. In case of rectangular/square and parallel channel pore scaffold, the direction of loading is same as the direction of the collagen filament in the patterned scaffold which helps the scaffold to withstand greater load. Conversely, collagen filaments are obliquely oriented to the loading direction in diamond-shaped pore which may have reduced the strength and the stiffness. Although the diamond-shaped pore may be weak in tensile direction, they may perform better where uniform load distribution is required due to the angular filament distribution. Parallel channel pore showed intermediate failure load due to the weak points which arose from lack of alignment in the interconnections between filaments.

The connected macroporosity of the scaffolds facilitated cell-seeding. Cells populated the entire scaffold at the time of seeding. After 3 days of culture, cell nuclei became elongated with an aspect ratio of 2.15. Native tendon, ligament, cardio myocyte and muscle cell has elongated nucleus with nucleus aspect ratio ranging from 2- 6 which is important in promoting a tenogenic, myogenic and ligament phenotypesM[5, 11, 33, 34, 40, 60]. The observed elongation of cell morphology may be beneficial in engineering such tissues using the proposed scaffold concept.

Unification of mechanical robustness with ample amount of macroporosity renders the electrocompacted collagen scaffolds for mesh-based applications which require rapid tissue ingrowth and neovascularization. Such applications include hernia repair, stress urinary incontinence (SUI), vaginal prolapse, thoracic wall reconstruction and tendon tissue engineering. At the present, such applications use synthetic polymers (e.g. polypropylene, polytetrafluoroethylene, polyester, etc.) autografts or decellularized allo/xenografts. Synthetic polymers provide acceptable mechanical properties. However they may present issues regarding cell adhesion[76, 77], systemic or local reactions [9, 10]. Biodegradable synthetic polymer scaffolds may be associated with foreign body giant cells[22].

To our knowledge pure collagen based scaffolds has not been used in clinical mesh application due to their weak mechanics [Table 1]. For clinical mesh application, to achieve mechanical robustness in collagen based scaffold, mostly collagen rich decellularized tissue such as small intestine submucosa (SIS), porcine acellular dermal matrix, and abdominal fascia (decellularized xenografts or allografts) were used[12, 58]. Decellularization may not always be fully effective and cell remnants may impact the scaffold host response, immune cell infiltration, tumor necrosis factor-α expression and macrophage activation[80]. Chemicals used in decellularization and radiation used for antigen deactivation results in damage to the

extracellular matrix which in turn may drive premature degradation of the implant before tissue integration takes place. The scaffold presented in this paper is a bottom-up fabrication sequence which utilizes pure collagen stock. Prior animal studies using electrocompacted threads demonstrated a high level of biocompatibility[38]. Therefore, incomplete removal of antigens is not a limitation for electrocompacted collagen. Moreover previous *in vitro* study of electrocompacted collagen showed favorable cell proliferation[4, 37] and differentiation[37] to tenogenic lineage. To the best of our knowledge, this is the first time a pure collagen scaffold mesh is reported within the mechanical strength range of decellularized tissue based xenografts [Table 1].

All of the aforementioned mesh based application requires mechanical robustness to a certain extent. Hernia repair meshes requires flexibility and optimized tensile strength to reduce discomfort. Polymer based meshes for hernia repair may be too strong and result in movement restriction and pain[18]. The tensile strength of a mesh required to withstand the maximum abdominal pressure is 32 N/cm[18] which is only a tenth of that of most meshes available now. High tensile strength polymers may be associated with erosion or extrusion in SUI repair[21]. The range of apparent tensile strength of existing xenograft and polypropylene sling products are 2-12 MPa and the apparent modulus range is 5-15 MPa[43]. Abdominal fascia used in autograft procedures in SUI application have a strength of up to 2 MPa and modulus of 10 MPa[36]. Polymer based meshes for thoracic diaphragm reconstruction has mechanical strength 25-40 N/cm[45]. However, thoracic reconstruction with synthetic materials are more prone to infection which necessitates costly removal procedure[51]. In the current study, six-layered scaffolds with different pore geometries have mechanical properties such as tensile stiffness, tensile strength and modulus ranges from 10-50 N/cm, 1-6 MPa and 5-40 MPa respectively which are within the range of practical usability of these applications. These patterned scaffolds also have porosity size ranging from 0.8-1.5 mm which is also within the range of most of the present repair meshes in the market. Moreover, the tensile strength can be optimized by changing the layer number of the scaffold, whenever optimization of tensile strength is required.

Conclusion

In summary, the current study developed a CAD/CAM based method to manufacture a pure collagen based highly porous patterned scaffold. High compaction and alignment of the collagen molecules rendered the construct mechanically robust. The results suggest that by changing the number of layers and shape of the structure, mechanical properties can be modulated for different tissue engineering application such as tendon, hernia, SUI, thoracic wall reconstruction.

The inability to incorporate high strength and high porosity in a structure is one of the major barriers in the engineering of load-bearing tissue, and the fabricated structure in this method addresses this limitation to some extent. This method utilizes computerized scaffold design and fabrication which allows the integration of ‘scaffolds with controlled porosity’. There is a general lack of biofabrication methods that will provide controlled porosity and the patterned electrochemical deposition method in this study has a potential to address this challenge at the fundamental level.

Acknowledgements

This study was funded in part by grants from the National Science Foundation (Grant Number DMR-1306665) and National Institute of Health (Grant Number R01 AR063701).

References

1. Abu-Rub MT, Billiar KL, van Es MH, Knight A, Rodriguez BJ, Zeugolis DI, et al. Nano-textured self-assembled aligned collagen hydrogels promote directional neurite guidance and overcome inhibition by myelin associated glycoprotein. Soft Matter. 2011; 7(6):2770–2781.
2. Agis H, Magdalenko M, Stogerer K, Watzek G, Gruber R. Collagen barrier membranes decrease osteoclastogenesis in murine bone marrow cultures. Clin Oral Implants Res. 2010; 21(6):656–61. [PubMed: 20337667]
3. Alberti KA, Xu Q. Slicing, stacking and rolling: fabrication of nanostructured collagen constructs from tendon sections. Adv Healthc Mater. 2013; 2(6):817–21. [PubMed: 23233344]
4. Alfredo Uquillas J, Kishore V, Akkus O. Genipin crosslinking elevates the strength of electrochemically aligned collagen to the level of tendons. J Mech Behav Biomed Mater. 2012; 15:176–89. [PubMed: 23032437]
5. Anversa P, Nadal-Ginard B. Myocyte renewal and ventricular remodelling. Nature. 2002; 415(6868):240–3. [PubMed: 11805849]
6. Bailin PL, Bailin MD, Bailin PL. Collagen Implantation: Clinical Applications and Lesion Selection. The Journal of Dermatologic Surgery and Oncology. 1988; 14:21–26. [PubMed: 3275700]
7. Barnard J, Millner R. A review of topical hemostatic agents for use in cardiac surgery. Ann Thorac Surg. 2009; 88(4):1377–83. [PubMed: 19766855]
8. Besner GE, Klamar JE. Integra Artificial Skin as a useful adjunct in the treatment of purpura fulminans. J Burn Care Rehabil. 1998; 19(4):324–9. [PubMed: 9710731]
9. Bostman O, Pihlajamaki H. Clinical biocompatibility of biodegradable orthopaedic implants for internal fixation: a review. Biomaterials. 2000; 21(24):2615–21. [PubMed: 11071611]
10. Bostman OM, Pihlajamaki HK. Adverse tissue reactions to bioabsorbable fixation devices. Clin Orthop Relat Res. 2000; (371):216–27. [PubMed: 10693569]
11. Bray MA, Adams WJ, Geisse NA, Feinberg AW, Sheehy SP, Parker KK. Nuclear morphology and deformation in engineered cardiac myocytes and tissues. Biomaterials. 2010; 31(19):5143–50. [PubMed: 20382423]
12. Brown C, Finch J. Which mesh for hernia repair? Ann R Coll Surg Engl. 2010; 92(4):272–8. [PubMed: 20501011]
13. Cavallo LM, Messina A, Esposito F, de Divitiis O, Dal Fabbro M, de Divitiis E, et al. Skull base reconstruction in the extended endoscopic transsphenoidal approach for suprasellar lesions. J Neurosurg. 2007; 107(4):713–20. [PubMed: 17937213]
14. TANGSADTHAKUN, Chalonglarp; S.K.; Neeracha SANCHAVANAKIT, TB.; DAMRONGSAKKUL, Siriporn. Properties of Collagen/Chitosan Scaffolds for Skin Tissue Engineering. Journal of Metals, Materials and Minerals. 2006; 16(1):37–44.
15. Chen G, Ushida T, Tateishi T. Scaffold Design for Tissue Engineering. Macromolecular Bioscience. 2002; 2(2):67–77.
16. Cheng X, Gurkan UA, Dehen CJ, Tate MP, Hillhouse HW, Simpson GJ, et al. An electrochemical fabrication process for the assembly of anisotropically oriented collagen bundles. Biomaterials. 2008; 29(22):3278–88. [PubMed: 18472155]
17. Choe JM, Kothandapani R, James L, Bowling D. Autologous, cadaveric, and synthetic materials used in sling surgery: comparative biomechanical analysis. Urology. 2001; 58(3):482–6. [PubMed: 11549510]
18. CN Brown JF. Which mesh for hernia repair? Ann R Coll Surg Eng. 2010; 92(4):272–278.
19. Cooper ML, Hansbrough JF, Spielvogel RL, Cohen R, Bartel RL, Naughton G. In vivo optimization of a living dermal substitute employing cultured human fibroblasts on a

biodegradable polyglycolic acid or polyglactin mesh. Biomaterials. 1991; 12(2):243–8. [PubMed: 1652296]

20. Cross VL, Zheng Y, Won Choi N, Verbridge SS, Sutermaster BA, Bonassar LJ, et al. Dense type I collagen matrices that support cellular remodeling and microfabrication for studies of tumor angiogenesis and vasculogenesis in vitro. Biomaterials. 2010; 31(33):8596–607. [PubMed: 20727585]
21. Daneshgari F, Kong W, Swartz M. Complications of mid urethral slings: important outcomes for future clinical trials. J Urol. 2008; 180(5):1890–7. [PubMed: 18801499]
22. Derwin KA, Codsi MJ, Milks RA, Baker AR, McCarron JA, Iannotti JP. Rotator cuff repair augmentation in a canine model with use of a woven poly-L-lactide device. J Bone Joint Surg Am. 2009; 91(5):1159–71. [PubMed: 19411465]
23. Dimitriou R, Mataliotakis G, Calori G, Giannoudis P. The role of barrier membranes for guided bone regeneration and restoration of large bone defects: current experimental and clinical evidence. BMC Medicine. 2012; 10(1):81. [PubMed: 22834465]
24. Elson ML. The Role of Skin Testing in the Use of Collagen Injectable Materials. The Journal of Dermatologic Surgery and Oncology. 1989; 15(3):301–303. [PubMed: 2783212]
25. Ford CN, Bless DM, Loftus JM. Role of injectable collagen in the treatment of glottic insufficiency: a study of 119 patients. Ann Otol Rhinol Laryngol. 1992; 101(3):237–47. [PubMed: 1543333]
26. Grover CN, Cameron RE, Best SM. Investigating the morphological, mechanical and degradation properties of scaffolds comprising collagen, gelatin and elastin for use in soft tissue engineering. J Mech Behav Biomed Mater. 2012; 10:62–74. [PubMed: 22520419]
27. Grunert P, Borde BH, Hudson KD, Macielak MR, Bonassar LJ, Hartl R. Annular repair using high-density collagen gel: a rat-tail in vivo model. Spine (Phila Pa 1976). 2014; 39(3):198–206. [PubMed: 24253790]
28. Harley BA, Leung JH, Silva EC, Gibson LJ. Mechanical characterization of collagen-glycosaminoglycan scaffolds. Acta Biomater. 2007; 3(4):463–74. [PubMed: 17349829]
29. Harris LD, Kim BS, Mooney DJ. Open pore biodegradable matrices formed with gas foaming. J Biomed Mater Res. 1998; 42(3):396–402. [PubMed: 9788501]
30. Haugh MG, Murphy CM, O'Brien FJ. Novel freeze-drying methods to produce a range of collagen-glycosaminoglycan scaffolds with tailored mean pore sizes. Tissue Eng Part C Methods. 2010; 16(5):887–94. [PubMed: 19903089]
31. Hollister SJ. Porous scaffold design for tissue engineering. Nat Mater. 2005; 4(7):518–24. [PubMed: 16003400]
32. Hutmacher DW. Scaffolds in tissue engineering bone and cartilage. Biomaterials. 2000; 21(24): 2529–43. [PubMed: 11071603]
33. Kajstura J, Urbanek K, Perl S, Hosoda T, Zheng H, Ogorek B, et al. Cardiomyogenesis in the adult human heart. Circ Res. 2010; 107(2):305–15. [PubMed: 20522802]
34. Kannus P. Structure of the tendon connective tissue. Scand J Med Sci Sports. 2000; 10(6):312–20. [PubMed: 11085557]
35. Kim TG, Chung HJ, Park TG. Macroporous and nanofibrous hyaluronic acid/collagen hybrid scaffold fabricated by concurrent electrospinning and deposition/leaching of salt particles. Acta Biomater. 2008; 4(6):1611–9. [PubMed: 18640884]
36. Kirilova M, Stoytchev S, Pashkouleva D, Kavardzhikov V. Experimental study of the mechanical properties of human abdominal fascia. Medical Engineering & Physics. 2011; 33(1):1–6. [PubMed: 21095153]
37. Kishore V, Bullock W, Sun X, Van Dyke WS, Akkus O. Tenogenic differentiation of human MSCs induced by the topography of electrochemically aligned collagen threads. Biomaterials. 2012; 33(7):2137–44. [PubMed: 22177622]
38. Kishore V, Uquillas JA, Dubikovsky A, Alshehabat MA, Snyder PW, Breur GJ, et al. In vivo response to electrochemically aligned collagen bioscaffolds. Journal of Biomedical Materials Research Part B: Applied Biomaterials. 2012; 100B(2):400–408. [PubMed: 22179969]
39. Kiyotani T, Teramachi M, Takimoto Y, Nakamura T, Shimizu Y, Endo K. Nerve regeneration across a 25-mm gap bridged by a polyglycolic acid-collagen tube: a histological and

electrophysiological evaluation of regenerated nerves. Brain Res. 1996; 740(1-2):66–74. [PubMed: 8973799]

40. Lee JY, Zhou Z, Taub PJ, Ramcharan M, Li Y, Akinbiyi T, et al. BMP-12 Treatment of Adult Mesenchymal Stem Cells *In Vitro* Augments Tendon-Like Tissue Formation and Defect Repair *In Vivo*. PLoS ONE. 2011; 6(3):e17531. [PubMed: 21412429]
41. Malda J, Woodfield TB, van der Vloodt F, Kooy FK, Martens DE, Tramper J, et al. The effect of PEGT/PBT scaffold architecture on oxygen gradients in tissue engineered cartilaginous constructs. Biomaterials. 2004; 25(26):5773–80. [PubMed: 15147823]
42. Malda J, Woodfield TB, van der Vloodt F, Wilson C, Martens DE, Tramper J, et al. The effect of PEGT/PBT scaffold architecture on the composition of tissue engineered cartilage. Biomaterials. 2005; 26(1):63–72. [PubMed: 15193881]
43. Mangera A, Bullock AJ, Chapple CR, Macneil S. Are biomechanical properties predictive of the success of prostheses used in stress urinary incontinence and pelvic organ prolapse? A systematic review. Neurourol Urodyn. 2012; 31(1):13–21. [PubMed: 22038890]
44. Martin R, Farjanel J, Eichenberger D, Colige A, Kessler E, Hulmes DJ, et al. Liquid crystalline ordering of procollagen as a determinant of three-dimensional extracellular matrix architecture. J Mol Biol. 2000; 301(1):11–7. [PubMed: 10926488]
45. Medical, G. http://www.goremedical.com/resources/dam/assets/AR2659-EN1.pdf
46. Micol LA, Arenas da Silva LF, Geutjes PJ, Oosterwijk E, Hubbell JA, Feitz WF, et al. Invivo performance of high-density collagen gel tubes for urethral regeneration in a rabbit model. Biomaterials. 2012; 33(30):7447–55. [PubMed: 22795859]
47. Miki H, Ando N, Ozawa S, Sato M, Hayashi K, Kitajima M. An artificial esophagus constructed of cultured human esophageal epithelial cells, fibroblasts, polyglycolic acid mesh, and collagen. ASAIO J. 1999; 45(5):502–8. [PubMed: 10503633]
48. Mikos AG, Bao Y, Cima LG, Ingber DE, Vacanti JP, Langer R. Preparation of poly(glycolic acid) bonded fiber structures for cell attachment and transplantation. Journal of Biomedical Materials Research. 1993; 27(2):183–189. [PubMed: 8382203]
49. Mikos AG, Sarakinos G, Leite SM, Vacant JP, Langer R. Laminated three-dimensional biodegradable foams for use in tissue engineering. Biomaterials. 1993; 14(5):323–330. [PubMed: 8507774]
50. Mikos AG, Thorsen AJ, Czerwonka LA, Bao Y, Langer R, Winslow DN, et al. Preparation and characterization of poly(l-lactic acid) foams. Polymer. 1994; 35(5):1068–1077.
51. Miller DL, Force SD, Pickens A, Fernandez FG, Luu T, Mansour KA. Chest wall reconstruction using biomaterials. Ann Thorac Surg. 2013; 95(3):1050–6. [PubMed: 23333060]
52. Mooney DJ, Baldwin DF, Suh NP, Vacanti JP, Langer R. Novel approach to fabricate porous sponges of poly(D,L-lactic-co-glycolic acid) without the use of organic solvents. Biomaterials. 1996; 17(14):1417–22. [PubMed: 8830969]
53. Nam YS, Park TG. Porous biodegradable polymeric scaffolds prepared by thermally induced phase separation. J Biomed Mater Res. 1999; 47(1):8–17. [PubMed: 10400875]
54. Narotam PK, Jose S, Nathoo N, Taylon C, Vora Y. Collagen matrix (DuraGen) in dural repair: analysis of a new modified technique. Spine (Phila Pa 1976). 2004; 29(24):2861–7. discussion 2868-9. [PubMed: 15599291]
55. Newton D, Mahajan R, Ayres C, Bowman JR, Bowlin GL, Simpson DG. Regulation of material properties in electrospun scaffolds: Role of cross-linking and fiber tertiary structure. Acta Biomater. 2009; 5(1):518–29. [PubMed: 18676212]
56. O'Brien FJ, Harley BA, Yannas IV, Gibson L. Influence of freezing rate on pore structure in freeze-dried collagen-GAG scaffolds. Biomaterials. 2004; 25(6):1077–86. [PubMed: 14615173]
57. Ochoa I, Pena E, Andreu EJ, Perez-Ilzarbe M, Robles JE, Alcaine C, et al. Mechanical properties of cross-linked collagen meshes after human adipose derived stromal cells seeding. J Biomed Mater Res A. 2011; 96(2):341–8. [PubMed: 21171153]
58. Pui CL, Tang ME, Annor AH, Ebersole GC, Frisella MM, Matthews BD, et al. Effect of repetitive loading on the mechanical properties of biological scaffold materials. J Am Coll Surg. 2012; 215(2):216–28. [PubMed: 22521670]

59. Qi Chen AB, Clarke Kieran, Carr Carolyn, Czernuszka Jan. Collagen-Based Scaffolds for Potential Application of Heart Valve Tissue Engineering. Tissue Science & Engineering. 2012; S11(003)
60. Stanley, Rachael L.; Janet, RF.; Patterson-Kane, C.; Goodship, Allen E.; Ralphs, Jim R. Confocal Microscopy and Image Analysis of Connexin Plaques in Equine Tendon. MICROSCOPY AND ANALYSIS. 2006
61. Rho KS, Jeong L, Lee G, Seo BM, Park YJ, Hong SD, et al. Electrospinning of collagen nanofibers: effects on the behavior of normal human keratinocytes and early-stage wound healing. Biomaterials. 2006; 27(8):1452–61. [PubMed: 16143390]
62. Roeder BA, Kokini K, Sturgis JE, Robinson JP, Voytik-Harbin SL. Tensile mechanical properties of three-dimensional type I collagen extracellular matrices with varied microstructure. J Biomech Eng. 2002; 124(2):214–22. [PubMed: 12002131]
63. Rosselli JE, Martins DM, Martins JL, Oliveira CR, Fagundes DJ, Taha MO. The effect of simvastatin on the regeneration of surgical cavities in the femurs of rabbits. Acta Cir Bras. 2014; 29(2):87–92. [PubMed: 24604311]
64. Ryan CM, Schoenfeld DA, Malloy M, Schulz JT 3rd, Sheridan RL, Tompkins RG. Use of Integra artificial skin is associated with decreased length of stay for severely injured adult burn survivors. J Burn Care Rehabil. 2002; 23(5):311–7. [PubMed: 12352131]
65. Saito, E.; Partee, B.; Das, S.; Hollister, SJ. Engineered wavy fibered polycaprolactone soft tissue scaffolds: design, fabrication and mechanical testing. 51st Orthopaedic Research Society Meeting; 2005. p. 51
66. Schoof H, Apel J, Heschel I, Rau G. Control of pore structure and size in freeze-dried collagen sponges. J Biomed Mater Res. 2001; 58(4):352–7. [PubMed: 11410892]
67. Schugens C, Maquet V, Grandfils C, Jerome R, Teyssie P. Biodegradable and macroporous polylactide implants for cell transplantation: 1. Preparation of macroporous polylactide supports by solid-liquid phase separation. Polymer. 1996; 37(6):1027–1038.
68. Schugens C, Maquet V, Grandfils C, Jerome R, Teyssie P. Polylactide macroporous biodegradable implants for cell transplantation. II. Preparation of polylactide foams by liquid-liquid phase separation. Journal of Biomedical Materials Research. 1996; 30(4):449–461. [PubMed: 8847353]
69. Sherwood JK, Riley SL, Palazzolo R, Brown SC, Monkhouse DC, Coates M, et al. A three-dimensional osteochondral composite scaffold for articular cartilage repair. Biomaterials. 2002; 23(24):4739–51. [PubMed: 12361612]
70. Spelzini F, Manodoro S, Frigerio M, Nicolini G, Maggioni D, Donzelli E, et al. Stem cell augmented mesh materials: an in vitro and in vivo study. Int Urogynecol J. 2015; 26(5):675–83. [PubMed: 25416022]
71. Sundaram CP, Keenan AC. Evolution of hemostatic agents in surgical practice. Indian J Urol. 2010; 26(3):374–8. [PubMed: 21116358]
72. Takahashi K. Effect of new bone substitute materials consisting of collagen and tricalcium phosphate. Bull Tokyo Dent Coll. 2009; 50(1):1–11. [PubMed: 19622874]
73. Tal H, Kozlovsky A, Artzi Z, Nemcovsky CE, Moses O. Cross-linked and non-cross-linked collagen barrier membranes disintegrate following surgical exposure to the oral environment: a histological study in the cat. Clin Oral Implants Res. 2008; 19(8):760–6. [PubMed: 18720556]
74. Uquillas J, Akkus O. Modeling the Electromobility of Type-I Collagen Molecules in the Electrochemical Fabrication of Dense and Aligned Tissue Constructs. Annals of Biomedical Engineering. 2012; 40(8):1641–1653. [PubMed: 22314838]
75. Uquillas JA, Kishore V, Akkus O. Effects of phosphate-buffered saline concentration and incubation time on the mechanical and structural properties of electrochemically aligned collagen threads. Biomed Mater. 2011; 6(3):035008. [PubMed: 21540522]
76. van Wachem PB, Beugeling T, Feijen J, Bantjes A, Detmers JP, van Aken WG. Interaction of cultured human endothelial cells with polymeric surfaces of different wettabilities. Biomaterials. 1985; 6(6):403–8. [PubMed: 4084642]
77. Wan Y, Chen W, Yang J, Bei J, Wang S. Biodegradable poly(L-lactide)-poly(ethylene glycol) multiblock copolymer: synthesis and evaluation of cell affinity. Biomaterials. 2003; 24(13):2195–203. [PubMed: 12699655]

78. Whang K, Thomas CH, Healy KE, Nuber G. A novel method to fabricate bioabsorbable scaffolds. Polymer. 1995; 36(4):837–842.

79. Woodfield TB, Malda J, de Wijn J, Peters F, Riesle J, van Blitterswijk CA. Design of porous scaffolds for cartilage tissue engineering using a three-dimensional fiber-deposition technique. Biomaterials. 2004; 25(18):4149–61. [PubMed: 15046905]

80. Xu H, Wan H, Sandor M, Qi S, Ervin F, Harper JR, et al. Host response to human acellular dermal matrix transplantation in a primate model of abdominal wall repair. Tissue Eng Part A. 2008; 14(12):2009–19. [PubMed: 18593339]

81. Younesi M, Islam A, Kishore V, Anderson JM, Akkus O. Tenogenic Induction of Human MSCs by Anisotropically Aligned Collagen Biotextiles. Advanced Functional Materials. 2014; 24(36): 5762–5770. [PubMed: 25750610]

82. Zorn KC, Spiess PE, Singh G, Orvieto MA, Moore B, Corcos J. Long-term tensile properties of tension-free vaginal tape, suprapubic arc sling system and urethral sling in an in vivo rat model. J Urol. 2007; 177(3):1195–8. [PubMed: 17296444]

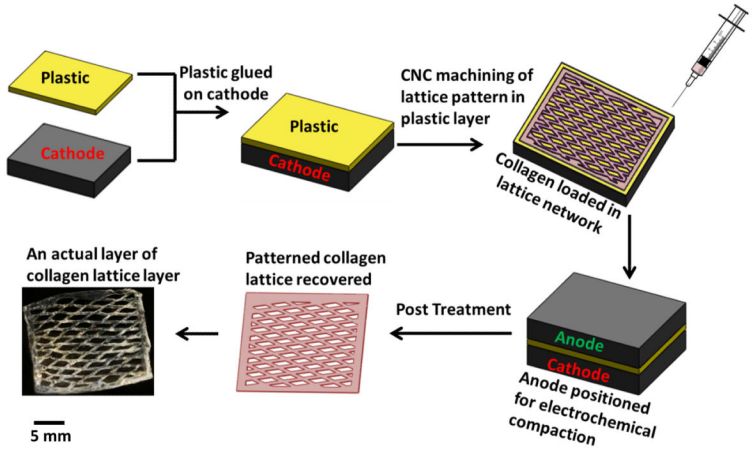

Figure 1.

Process of fabricating individual patterned layer. Patterned electrochemical compaction of monomeric collagen solutions as mechanically robust lattice layers. The layers can be stacked to obtain thicker scaffolds.

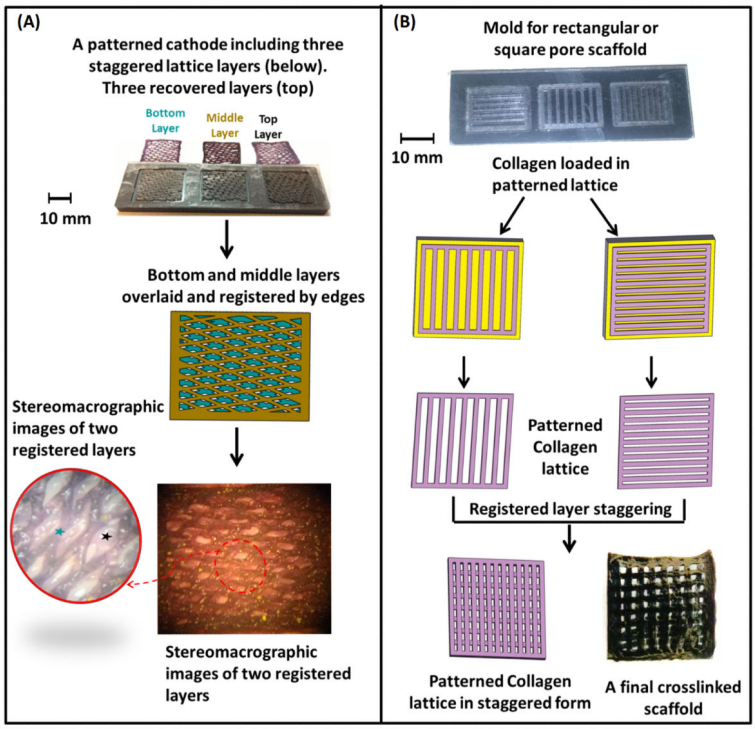

Figure 2.

3D-scaffolds can be obtained by overlaying the individual lattice layers. The pore network is staggered between each consecutive layer to attain interconnected porosity. The registration of the stagger pattern is accounted for during the CNC based machining of the electrode system. A) 3D-interconnected porosity can be attained by overlaying multiple layers while staggering the pore structure. Blue and black ‘ ★ ’ denote the two separate scaffold layers. B) Layers can be patterned as parallel channel to induce collagen molecule alignment and make desired pore shaped scaffolds by staggering the individual layers.

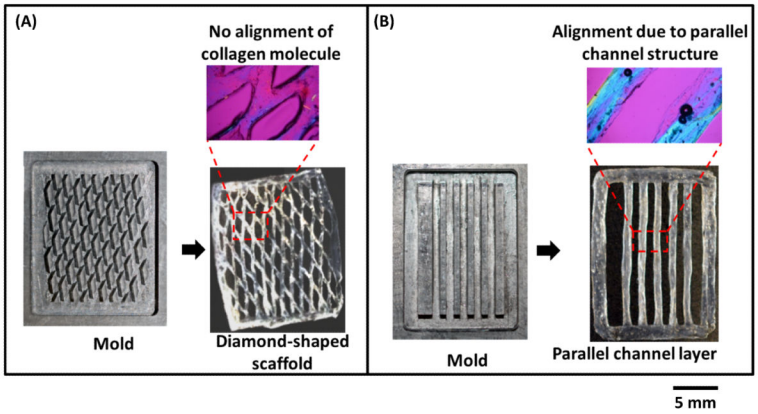

Figure 3.

A) Branching in the diamond-shaped patterned lattice displayed lack of alignment of collagen molecules as manifested by the magenta in the compensated polarize image (CPI). B) Parallel channels introduce alignment in the patterned layer (emergence of blue color in CPI indicates alignment).

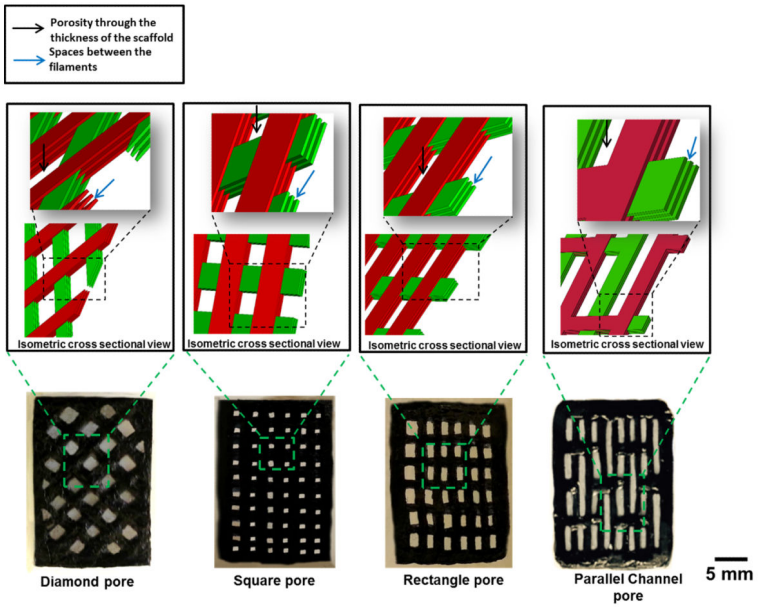

Figure 4.

Scaffolds with 4 different porosity shapes. A) Diamond-shaped pore; B) Square-shaped pore; C) Rectangle-shaped pore 4) Parallel channel pore. Black color of the scaffolds are due to genipin cross linking. Black arrow indicates porosity through the thickness of the scaffold and blue arrow indicates spaces between the filaments of the layers of the scaffold.

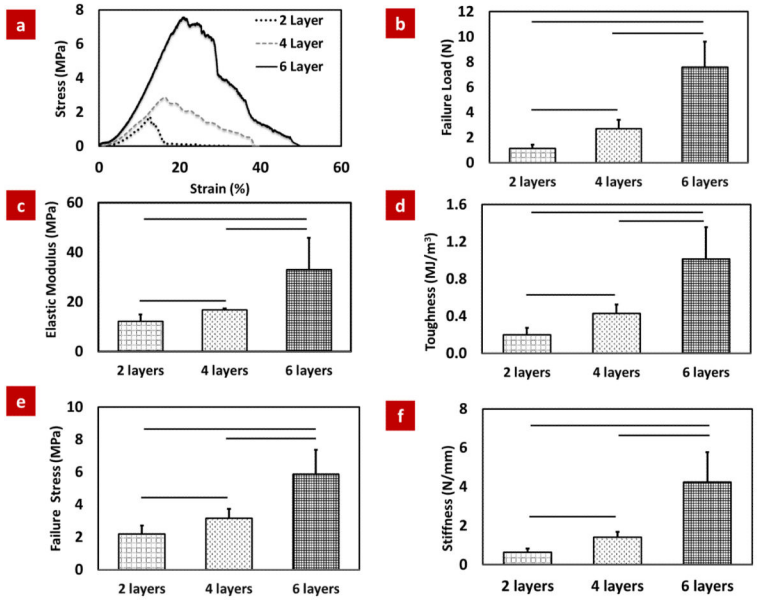

Figure 5.

Mechanical assessment of patterned scaffolds with three different layer numbers. (a) Typical stress-strain curves for different layer scaffolds, (b) Failure load, (c) Elastic modulus, (d) Toughness (e) Failure stress and (f) Stiffness of 6 layer scaffold is more than 3 fold greater than the 2 layer scaffolds. The horizontal line indicates significant difference ($p < 0.05$).

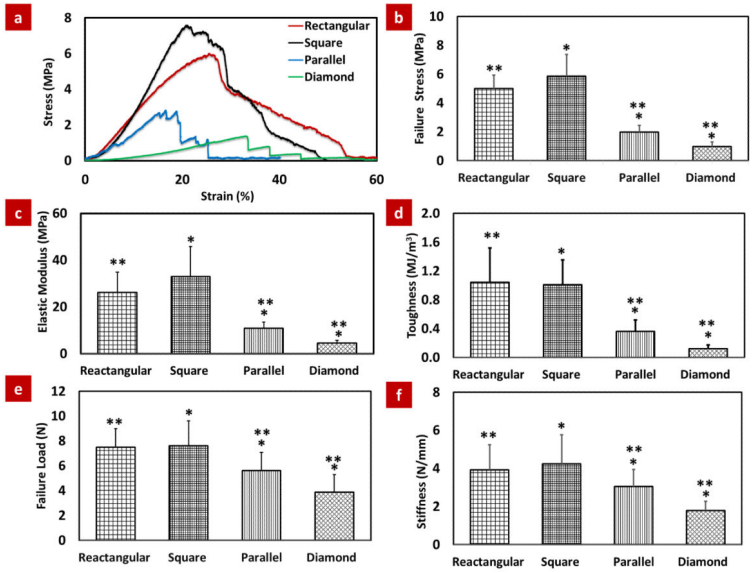

Figure 6.

Mechanical assessment of patterned scaffolds with four different pore shapes. (a) Typical stress-strain curves for different porosity scaffolds, (b) Failure stress, (c) Elastic modulus, (d) Toughness (e) Failure load and (f) Stiffness of rectangular/square-shaped pore scaffolds were highest, parallel channel pore scaffolds were intermediate and diamond-shaped pore scaffolds were lowest. Asterisks indicate significant differences between groups ($p < 0.05$).

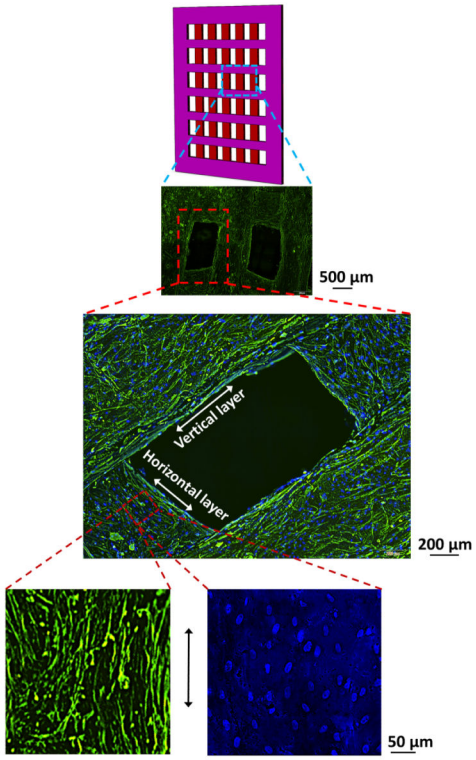

Figure 7.

DAPI (blue) and F-Actin (green) staining images revealed that cells covered the entire scaffold through thickness. Cells and nucleus became elongated along the length of the collagen filament (bottom enlarged image - horizontal direction).

Table 1

Comparative mechanical properties of collagen based scaffolds for tissue engineering application

Collagen Based Scaffold		Market Name	Compressive Modulus	Compressive Strength	Tensile Strength	Elastic Modulus
Collagen rich xenografts (decellularized collagen matrix)	Porcine dermis	Permacol[58]			38 MPa	210 MPa
		CollaMend[58]			10MPa	30 MPa
		Strattice[58]			15 MPa	50 MPa
		XenMatrix[58]			12 MPa	40MPa
		Pelvitex[70]			1.2 MPa	5 MPa
	Human dermis	FlexHD[58]			10MPa	30 MPa
		AlloMax[58]			22 MPa	60 MPa
	Bovine pericardium	Veritas[58]			6MPa	20 MPa
		PeriGuard[58]			16 MPa	110 MPa
	Porcine SIS	Surgisis[58, 70]			4 MPa	15 MPa
	Human abdominal fascia[36]				2 MPa	10 MPa
	Porcine dermis[57]					0.2 -3.5 MPa
	Animal SIS	Strasis[82]			3 MPa	
	Human cadaveric dermis	Alloderm[17]			7.2 MPa	
	Human cadaveric fascia lata	Faslata[17]			10.85 MPa	
	Decellularized tendon section (Sheet form) [3]				0.2-0.7 MPa	0.5- 6 MPa
Pure collagen (reconstituted collagen)	**Electrocompacted patterned scaffolds in this study**				**1-6 MPa**	**5-40 MPa**
	Gel form (dogbone shape) [3]				0.1 MPa	0.2 MPa
	Electrospun Collagen[55]				0.3 MPa	0.4 MPa
	Collagen, Collagen+ Elastin (freeze dry) [59]		25 kPa	12 kPa	80 kPa	350-200 kPa
	Collagen freeze dry[26]				7.8 kPa	81 kPa
	Collagen–glycosaminoglycan (freeze dry) [28]				5.1 kPa	30 kPa
	Gel form (dog bone shape) [62]				0.5-9 kPa	1.54-25 kPa
	Collagen (freeze dry) [14]		20 kPa			
	Collagen-chitosan (freeze dry) [14]		10-20 kPa			